JOURNAL OF MECHANICS OF CONTINUA AND MATHEMATICAL SCIENCES
www.journalimcms.org

ISSN (Online) : 2454 -7190 Vol.-18, No.-11, November (2023) pp 31-41 ISSN (Print) 0973-8975

NATURAL CONVECTION IN A POROUS MEDIUM SATURATED BY NANOFLUID WITH MODIFIED BOUNDARY CONDITION – ARTIFICIAL NEURAL NETWORK (ANN) APPROACH

Asish Mitra[1], Dilip Kumar Gayen[2]

[1] Department of Basic Sciences. College of Engineering & Management, Kolaghat, West Bengal, India

[2] Department of Computer Science And Engineering
College of Engineering & Management, Kolaghat, West Bengal, India

Corresponding author: **Dilip Kumar Gayen**

Email: [1]asish@cemk.ac.in, [2]dilipgayen@cemk.ac.in

https://doi.org/10.26782/jmcms.2023.11.00003

(Received: September 20, 2023; Revised: November 5, 2023; Accepted: November 21, 2023)

Abstract

In the present numerical study, steady, laminar, two-dimensional flow in a porous medium saturated by nanofluid along an isothermal vertical plate is covered. Here we have considered a realistic situation where the nanoparticle volume fraction at the plate surface (boundary condition) is passively controlled by assuming that its flux there is zero. We make use of the Buongiorno model that treats the nanofluid as a two-component mixture, incorporating the effects of Brownian motion and thermophoresis. The Darcy model is employed for the porous medium. By suitable similarity variables, the governing nonlinear partial differential equations of flow are altered to a bunch of nonlinear ordinary differential equations. They have been transformed into a first-order system afterward and then integrated using Newton Raphson and adaptive Runge-Kutta methods. The computer codes are produced for this mathematical investigation in a Matlab environment. To accurately predict major parameters (reduced Nusselt number, Nur, Thermophoresis parameter, Nt Brownian motion parameter, Nb and buoyancy-ratio parameter, Nr), an artificial neural network (ANN) is developed, trained, and tested by numerically simulated data. The dependence of the reduced Nusselt number on these parameters is represented through a linear regression correlation.

Keywords: Artificial Neural Network, Brownian Motion, Isothermal Vertical Plate, Natural Convection, Nanofluid, Porous Medium, Thermophoresis.

I. Introduction

Nanofluids are a moderately new class of liquids that comprise a base liquid with nano-sized particles (1 - 100 nm) suspended. It was introduced by Choi in 1995. Nanofluids have novel properties that make them potentially useful in many

applications in heat transfer: transportation (engine cooling/vehicle thermal management), nuclear system cooling, electronics cooling, solar water heating, heat exchangers, biomedicine, fuel cells, etc. Nanofluid in porous media is an emerging topic, as heat transfer efficiency is optimized by porous media. Cheng and Minkowycz [VIII] studied similar solutions for free convective heat transfer from a vertical plate in a fluid-saturated porous medium. Gorla and Tornabene [X] and Gorla and Zinolabedini [XI] tackled issues of free convective heat transfer from a vertical plate embedded in a saturated porous medium with constant, arbitrarily varying surface temperature or heat flux. The issue of combined convection from vertical plates in porous media was investigated by Minkowycz et al. [XIV] and Ranganathan and Viskanta [IX]. All of these studies were concerned with Newtonian fluid flows. The boundary layer flows in nanofluids have been analyzed recently by [II, III].

The main purpose of this study is to analyze the effect of physical parameters associated with the steady, laminar, two-dimensional flow in a porous medium saturated by nanofluid along an isothermal vertical plate by using an artificial neural network. The newly introduced boundary condition of zero mass flux of nanoparticles at the plate is an added feature to the novelty of the problem.

II. Mathematical Model

We assume the natural convection flow to be steady, laminar, and two-dimensional. We take the direction along the vertical plate to be x, and the direction normal to the surface to be y (Fig 1).

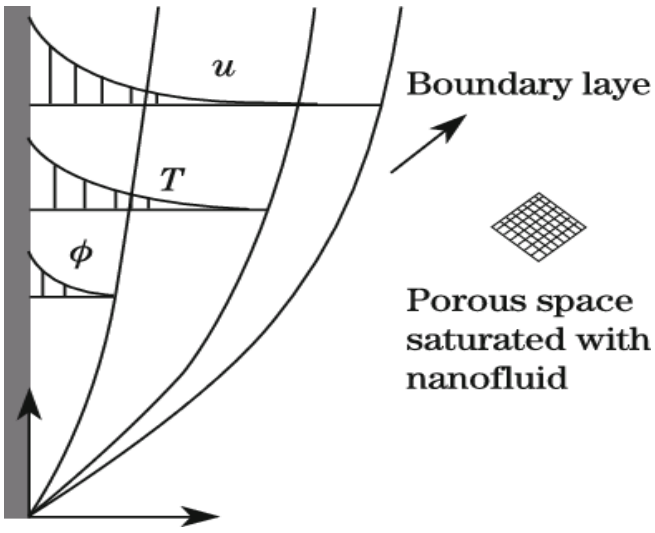

Fig. 1. Physical Model

Following Oberbeck-Boussinesq approximation and standard boundary layer approximations, the equations governing the flow [8] are:

$$\frac{\partial u}{\partial x} + \frac{\partial v}{\partial x} = 0 \qquad (1)$$

$$\frac{\partial p}{\partial x} = -\frac{\mu}{K}u + [(1-\varphi_\infty)\rho_{f\infty}\beta g(T-T_\infty) - (\rho_p - \rho_{f\infty})g(\varphi-\varphi_\infty)] \quad (2)$$

$$\frac{\partial p}{\partial y} = 0 \quad (3)$$

$$u\frac{\partial T}{\partial x} + v\frac{\partial T}{\partial y} = \alpha_m \nabla^2 \mathrm{T} + \tau[\mathrm{D_B}\frac{\partial \varphi}{\partial y}\frac{\partial T}{\partial y} + (\frac{\mathrm{D_T}}{\mathrm{T_\alpha}})(\frac{\partial T}{\partial y})^2] \quad (4)$$

$$\frac{1}{\varepsilon}(u\frac{\partial \varphi}{\partial x} + v\frac{\partial \varphi}{\partial y}) = \mathrm{D_B}\frac{\partial^2 \varphi}{\partial y^2} + (\frac{\mathrm{D_T}}{\mathrm{T_\alpha}})\frac{\partial^2 T}{\partial y^2}] \quad (5)$$

$$\alpha_m = \frac{k_m}{(\rho c)_f}, \qquad \tau = \frac{\varepsilon(\rho c)_p}{(\rho c)_f} \quad (6)$$

where Darcy velocity components along x and y are represented by u and v, respectively, T_∞ and φ_∞ are temperature and nanoparticle volume fractions far away from the plate respectively, ρ_f, μ, and β are the density, viscosity and volumetric thermal expansion coefficient of the fluid, ρ_p is the density of the nanoparticles, k_m and $(\rho c)_m$ are effective thermal conductivity and effective heat capacity of the porous medium respectively. g is the acceleration due to gravity, $(\rho c)_f$ is the heat capacity of the fluid, $(\rho c)_p$ is the effective heat capacity of the nanoparticle material, D_B and D_T are the Brownian diffusion coefficient and thermophoretic diffusion coefficient, respectively. ε and K are the porosity and permeability of the porous medium. The boundary conditions on the solution are:

At y = 0: v = 0, T = T_w, $D_B\frac{\partial \phi}{\partial y} + \frac{D_B}{T_\infty}\frac{\partial T}{\partial y} = 0$ (7) (a, b, c)

For large y: u= v = 0, T = T_∞ , $\varphi = \varphi_\infty$ (8) (a, b, c)

The last statement of (7c) indicates the modified boundary condition on nanoparticle volume fraction at the surface of the plate. It is redesigned such that its mass flux at the plate is zero. The congruity condition (1) is naturally fulfilled through the presentation of the stream function:

$$u = \frac{\partial \psi}{\partial y} \qquad v = -\frac{\partial \psi}{\partial x} \quad (9)$$

And, we can eliminate pressure p from equations (2) and (3) by cross-differentiation, and get the following equations from equations (2) to (5)

$$\frac{\partial^2 \psi}{\partial y^2} = \frac{(1-\varphi_\infty)\rho_{f\infty}\beta g K}{\mu}\frac{\partial T}{\partial y} - \frac{(\rho_p - \rho_{f\infty})gK}{\mu}\frac{\partial \varphi}{\partial y} \quad (10)$$

$$\frac{\partial \psi}{\partial y}\frac{\partial T}{\partial x} - \frac{\partial \psi}{\partial x}\frac{\partial T}{\partial y} = \alpha_m \nabla^2 \mathrm{T} + \tau[\mathrm{D_B}\frac{\partial \varphi}{\partial y}\frac{\partial T}{\partial y} + (\frac{\mathrm{D_T}}{\mathrm{T_\alpha}})(\frac{\partial T}{\partial y})^2] \quad (11)$$

$$\frac{1}{\varepsilon}\left(\frac{\partial\psi}{\partial y}\frac{\partial\varphi}{\partial x}-\frac{\partial\psi}{\partial x}\frac{\partial\varphi}{\partial y}\right)=\mathrm{D_B}\frac{\partial^2\varphi}{\partial y^2}+\left(\frac{\mathrm{D_T}}{\mathrm{T_\alpha}}\right)\frac{\partial^2 T}{\partial y^2}\Big] \tag{12}$$

With the introduction of the following similarity variables

$$\eta=\frac{y}{x}Ra_x^{1/2} \tag{13}$$

$$s(\eta)=\frac{\psi}{\alpha_m Ra_x^{1/2}} \tag{14}$$

$$\theta(\eta)=\frac{T-T_\infty}{T_w-T_\infty} \tag{15}$$

$$f(\eta)=\frac{\varphi-\varphi_\infty}{\varphi_\infty} \tag{16}$$

equations (10), (11), and (12) may be rewritten as (with a prime denoting differentiation concerning η)

$$s''-\theta'+Nrf'=0 \tag{17}$$

$$\theta''+\frac{1}{2}s\theta'+Nbf'\theta'+Nt\theta'^2=0 \tag{18}$$

$$f''+\frac{1}{2}Lesf'+\frac{Nt}{Nb}\theta''=0 \tag{19}$$

The appropriate boundary conditions are:

$$s=0,\ \theta=1,\ Nbf'+Nt\theta'=0 \quad \text{at } \eta=0 \tag{20 (a, b, c)}$$

$$s'=0,\ \theta=1,\ f=0 \text{ at } \eta=\infty \tag{21 (a, b, c)}$$

where Local Rayleigh number Ra_x, the buoyancy-ratio parameter (Nr), Brownian motion parameter (Nb), thermophoresis parameter (Nt), and Lewis number (Le) are defined as follows:

$$Ra_x=\frac{(1-\varphi_\infty)\rho_{f\infty}\beta gKx}{\mu\alpha_m} \tag{22}$$

$$Nr=\frac{(\rho_p-\rho_{f\infty})\varphi_\infty}{\rho_{f\infty}\beta(T_w-T_\infty)(1-\varphi_\infty)} \tag{23}$$

$$Nb=\frac{\varepsilon(\rho c)_p\mathrm{D_B}\varphi_\infty}{(\rho c)_f\alpha_m} \tag{24}$$

$$Nt = \frac{\varepsilon(\rho c)_p D_T (T_w - T_\infty)}{(\rho c)_f \alpha_m T_\infty} \tag{25}$$

$$Le = \frac{\alpha_m}{\varepsilon D_B} \tag{26}$$

Equation (17) after integration once with boundary conditions (21) gives

$$s' - \theta + Nrf = 0 \tag{27}$$

Associated boundary conditions are

$$\text{At } \eta \to \infty, \quad \theta = 0, f = 0 \tag{28 (a, b)}$$

Local Nusselt number is defined as

$$Nu = \frac{q'' x}{k_m (T_w - T_\infty)} \tag{29}$$

where q" is the wall heat flux. The reduced local Nusselt number is then

$$Nur = \frac{Nu}{Ra_x^{1/4}} = -\theta'(0) \tag{30}$$

III. Solution Procedure

Equations (27, 18, 19) are transformed to a first-order system and then integrated using Newton Raphson and adaptive Runge-Kutta methods. A detailed solution procedure is available in [I]. The solution to equations (27, 18, 19) gives the tabulated values of s, s', θ, θ', f, f' as functions of η with Le, Nr, Nb, and Nt are parameters. The set of discrete values of the parameters Le, Nr, Nb, and Nt of the present study used in the codes are given in Table 1.

Table 1 Values of input parameters

Input parameters	values
Le	1, 10, 100, 1000
Nr	0.1, 0.2, 0.3, 0.4, 0.5
Nb	0.1, 0.2, 0.3, 0.4, 0.5
Nt	0.1, 0.2, 0.3, 0.4, 0.5

Reduced Nusselt numbers for 125 sets of values of Nr, Nb, Nt in the range [0.1, 0.2, 0.3, 0.4, 0.5] with Le = 10 are obtained in tabular form in this procedure.

IV. Artificial Neural Network Approach

Artificial neural networks (ANNs) are breaking free from the constraints of conventional methodologies. Unlike traditional methods, ANNs do not depend on

specific structural prerequisites; they thrive on a wealth of input/output data. When meticulously trained, ANNs exhibit the remarkable ability to discern both linear and nonlinear relationships within input-output data [6, 7, 13, 4]. Their adaptability to new information is a product of continuous retraining. The first step in crafting an effective ANN algorithm revolves around the utilization of input-output data. This flexibility, enabled by the power of ANNs, not only enhances problem-solving but also opens new avenues for understanding complex data patterns, making them a valuable asset in various fields. This neural network is designed with three layers: the input layer, the output layer, and one or more hidden layers, as illustrated in Fig. 2. The input layer comprises three neurons representing the Brownian motion Parameter (Nb), thermophoresis parameter (Nt), and buoyancy-ratio parameter (Nr), which are inputs to the system. The output layer consists of a single neuron representing the Nusselt number (Nur). The dataset is divided into three parts: the training dataset, the validation dataset, and the testing dataset. The training dataset is used for training the neural network, and the network is adjusted based on its error. The validation dataset is employed to assess network generalization and determine when to halt training if generalization doesn't improve. The testing dataset is used to evaluate network performance during and after training. In this design, 85% of the total dataset is used for training, 10% for testing, and the remaining portion is for assessing network performance. Each neuron in the hidden layer is assigned weights (W_{Ij}) and biases (B_j), while each neuron in the output layer has weights (W_{jO}) and biases (B_O).

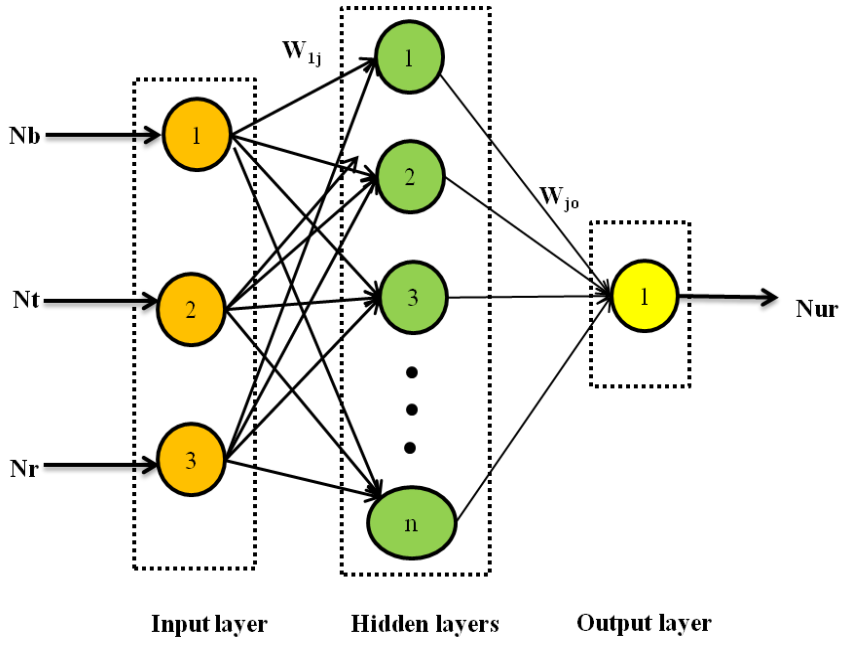

Fig. 2. Architecture of three layers of ANN

To determine the optimal hidden layer neuron count, we calculated the Mean Square Error (MSE) with the provided formula.

$$\text{Mean Square Error (MSE)} = \frac{1}{n}\sum_{k=1}^{n}(y_{tn} - y_{te})^2 \quad (31)$$

Here, 'n' represents the total dataset size, 'y_{te}' is the actual (target) output, and 'y_{tn}' is the ANN's output (predicted) after training. We've graphed the MSE with varying numbers of hidden layer neurons, as depicted in Fig. 3. Our objective is to identify the neuron count that results in the lowest MSE.

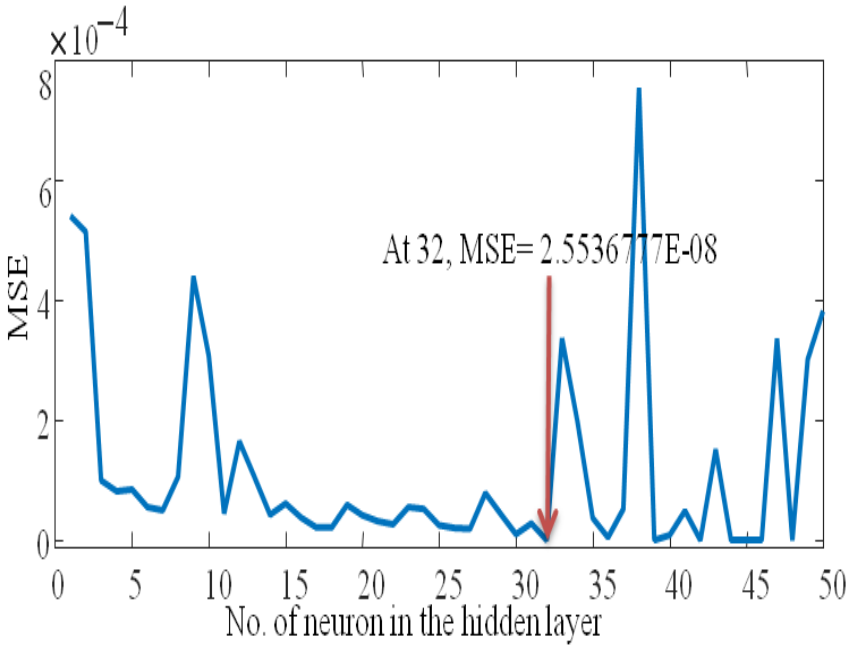

Fig. 3. MSE with the number of neurons in the hidden

Fig. 3 indicates that the lowest MSE is attained with 32 neurons. Thus, we selected 32 neurons for the hidden layer. MSE represents the average squared difference between predicted and target values, with smaller values being preferable. In this case, the MSE is 2.553E-08.

Fig. 4 illustrates the changes in MSE for the training, validation, and testing datasets across different epochs. It is evident that the best validation performance, 8.1043e-08, is achieved at epoch 11. However, beyond this point, increasing the number of iterations results in higher errors, necessitating a halt in training.

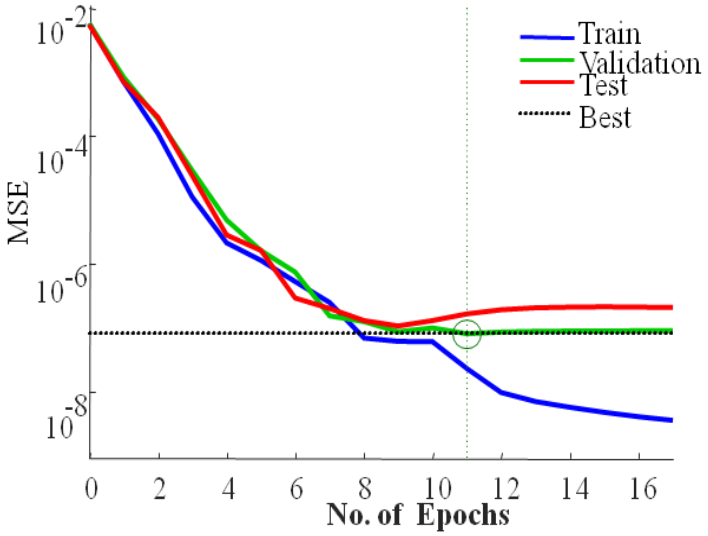

Fig. 4. Variation of MSE for training, validation, and testing data set with several Epochs.

The linear regression value is determined by assessing the correlation between results and targets. A value of 1 indicates a strong correlation, while 0 signifies a weak correlation. Fig. 5 displays the regression for various datasets (training, validation, testing, and overall). It's evident from the figures that the regression factor is close to 1, indicating a robust association between the input dataset and the modeled data in this neural network.

Correlation

With this trained network, we have now calculated expected output (Nur) values for several input data sets (Nb, Nt, and Nr). The linear regression, performed on the results, yielded a correlation.

$$Nur_{ANN} = 0.4433 - 0.0003Nr + 0.0007Nb - 0.1045Nt \quad (32)$$

with a maximum error of about 1%. This may be put side by side with the correlation where the nanoparticle volume fraction at the plate is actively controlled [II], which was

$$Nur_{est} = 0.444 - 0.111Nr - 0.245Nb - 0.150Nt \quad (33)$$

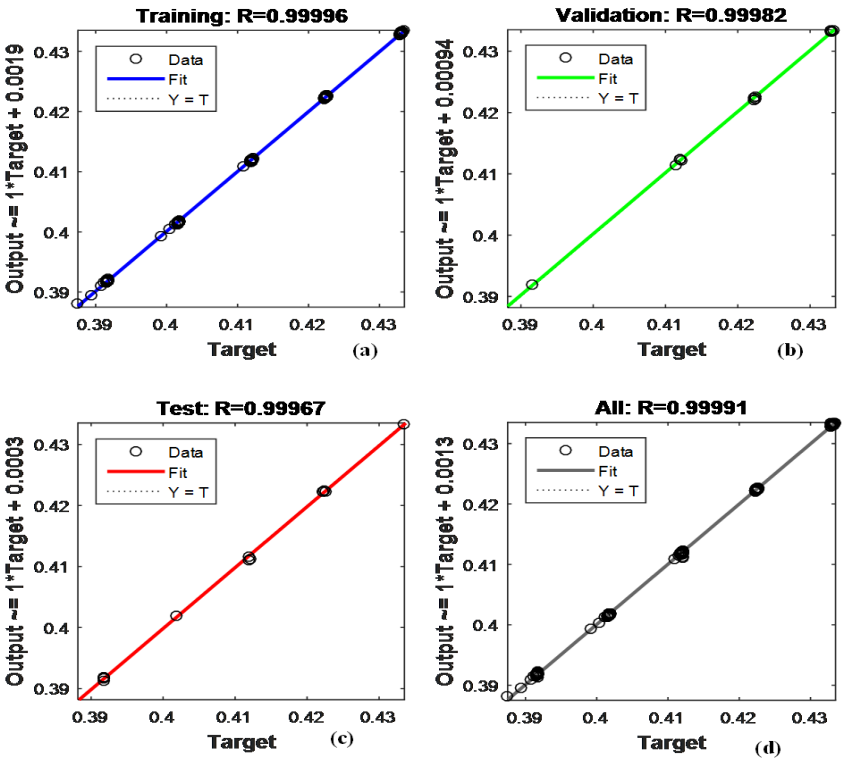

Fig. 5. Linear Regression Fit for Input Data and Modelled Data, (a) Training Dataset, (b) Validation Dataset, (c) Testing Dataset, and (d) Overall Dataset.

and had a maximum error of about 12%. With the modified boundary condition on nanoparticle volume fraction at the plate, Nur_{est} turns out to be almost independent of the Brownian motion parameter Nb and the buoyancy-ratio parameter (Nr) [eq. (32)], whereas these parameters have significant effects in the case of actively controlled nanoparticle volume fraction at the plate [eq (33)]. Eq (32) demonstrates the reduced Nusselt number decreases as the parameter Nt (thermophoresis parameter) increases, which increases the thermal boundary layer.

V. Conclusion and Outlook

In the present numerical study, steady, laminar, two-dimensional flow in a porous medium saturated by nanofluid along an isothermal vertical plate is presented. Here we have critically examined a more realistic situation where the nanoparticle volume fraction at the plate surface (boundary condition) is passively forced by assuming that its flux there is zero. We employ the Boungiorno model that treats the nanofluid as a two-component mixture, incorporating the effects of Brownian motion and thermophoresis. For the porous medium, the Darcy model is utilized. The solution to the governing equations is transformed into a first-order system and then integrated using Newton Raphson and adaptive Runge-Kutta methods and gives the

reduced Nusselt number as functions of the parameters Nr, Nb, and Nt. A linear regression correlation between them is also developed using the Artificial Neural Network approach. The reduced Nusselt number (Nur) is found to be a decreasing function of Nt (Thermophoresis parameter), and practically independent of Nb (Brownian motion parameter) and Nr (buoyancy-ratio parameter), whereas, in the case of actively controlled nanoparticle volume fraction at the plate, Nb and Nr have significant effects.

Conflict of Interest

The authors declare that they have no conflicts of interest to report regarding the present study.

References

I. A Mitra, : "Consequence of Modified Boundary Condition On Natural Convection in a Porous Medium Saturated by Nanofluid – A Computational Approach", IOP Conf. Series: Earth Environ. Sci., 1-9, 785, 2021.

II. D. A. Nield and A. V. Kuznetsov, : "The Cheng-Minkowycz Problem for Natural Convective Boundary Layer Flow in a Porous Medium Saturated by a Nanofluid." *International Journal of Heat and Mass Transfer*, vol. 52, pp. 5792–5795, 2009.

III. D. A. Nield and A. V. Kuznetsov, : "Thermal Instability in a Porous Medium Layer Saturated by a Nanofluid." *International Journal of Heat and Mass Transfer*. vol. 52, pp. 5796–5801, 2009.

IV. J. A. Ujong, E. M. Mbadike, and G. U. Alaneme, : "Prediction of cost and duration of building construction using artificial neural network", *Asian Journal of Civil Engineering*. 23, 1117–1139 (2022).

V. J. Buongiorno, : "Convective transport in nanofluids." *ASME J. Heat Transf.* 128 (2006) 240–250.

VI. K.-T. Yang, : "Artificial Neural Networks (ANNs): A New Paradigm for Thermal Science and Engineering", *Journal of Heat Transfer*. 130, 093001-1-19 (2008).

VII. M. H. Esfe, M. H. Kamyab and D. Toghraie, : "Statistical review of studies on the estimation of thermophysical properties of nanofluids using artificial neural network (ANN)." *Powder Technology*. 400, 117210 (2022).

VIII. P. Cheng, and W. J. Minkowycz, : "Free Convection about a Vertical Flat Plate Embedded in a Saturated Porous Medium with Applications to Heat Transfer from a Dike." *Journal of Geophysics Research*. vol. 82, pp. 2040–2044, 1977. 7.

IX. P. Ranganathan and R. Viskanta, : "Mixed Convection Boundary Layer Flow along a Vertical Surface in a Porous Medium." *Numerical Heat Transfer*. vol. 7, pp. 305–317, 1984.

X. R. S. R. Gorla and R. Tornabene, : "Free Convection from a Vertical Plate with Non-uniform Surface Heat Flux and Embedded in a Porous Medium." *Transport in Porous Media*. vol. 3, pp. 95–106, 1988.

XI. R. S. R. Gorla and A. Zinolabedini, : "Free Convection from a Vertical Plate with Nonuniform Surface Temperature and Embedded in a Porous Medium, Transactions of ASME." *Journal of Energy Resources Technology*. vol. 109, pp. 26–30, 1987.

XII. S. Choi, : "Enhancing thermal conductivity of fluids with nanoparticle in: D. A. Siginer, H. P. Wang (Eds.), Developments and Applications of Non-Newtonian Flows." *ASME MD vol. 231 and FED*. vol. 66, 1995, pp. 99–105.

XIII. V. Gholami and H. Sahour, : "Simulation of rainfall-runoff process using an artificial neural network (ANN) and field plots data", *Theoretical and Applied Climatology*. 147, 87–98 (2022).

XIV. W. J. Minkowycz, P. Cheng, and C.H. Chang, : "Mixed Convection about a Nonisothermal Cylinder and Sphere in a Porous Medium." *Numerical Heat Transfer*. vol. 8, pp. 349–359, 1985.